MODEL PREDICTIVE CONTROL OF A MODULAR MULTILEVEL CONVERTER WITH SIMPLIFIED CAPACITOR VOLTAGE BALANCING

LAÍS F. CRISPINO, LUÍS G. B. ROLIM

Power Electronics Laboratory, Electrical Engineering Department, Federal University of Rio de Janeiro
Caixa Postal 68504, 21941-972, Rio de Janeiro, RJ, Brasil
E-mails: laiscrispino@coe.ufrj.br, rolim@ufrj.br

Abstract— The operation and applications referred to the modular multilevel converter (MMC) have been a subject of increasing interest and research by the scientific community. However, the recently studied application areas for this converter topology are mainly high voltage dc transmission (HVDC), with medium/high power. This paper proposes to use a model predictive control (MPC) as a control strategy to regulate the ac-side currents and circulating currents. Also a suboptimal algorithm which uses a reduced number of considering states to implement the task of maintaining the submodules capacitor voltage balanced is proposed. The performance of this control strategy applied to a five-level MMC connected to the medium voltage distribution grid is analysed based on simulation results conducted in the environment of circuit simulations PSIM.

Keywords— MMC, Multilevel converters, Distributed Generation, MPC, Voltage Balancing.

Resumo— O funcionamento e aplicações referentes ao conversor multinível modular (CMM) vêm sendo, cada vez mais, objeto de interesse e pesquisa por parte da comunidade científica. Entretanto, as aplicações estudadas para essa nova topologia de conversor são, em sua maioria, sistemas de transmissão em corrente contínua de alta tensão (CCAT), de média/alta potência. Este trabalho propõe utilizar o modelo preditivo (MPC) como estratégia de controle para regular a corrente no lado CA, bem como as correntes circulantes no CMM. Ainda, é proposto um algoritmo sub-ótimo, e que considera um número reduzido de estados, para realizar a tarefa de balanceamento dos capacitores. A performance dessa estratégia de controle aplicada a um CMM de cinco níveis de tensão fase-neutro conectado à rede de média tensão, é avaliada com base em simulações feitas no ambiente de simulação de circuitos PSIM.

Palavras-chave— CMM, Conversores multinível, Geração Distribuída, MPC, Balanceamento das tensões.

1 Introduction

The Modular Multilevel Converter was first introduced in (Lesnicar, 2003), and since then it has been a subject of great interest in power electronics researches. This converter topology has been considered attractive in medium and high voltage applications since, as compared with the conventional two or three-level converters, they provide high power quality at the ac-side, higher output voltages with extremely low distortion and reduction in the device average switching frequency without compromise of power quality, which allows operation with lower switching frequency (Rodriguez, 2002) and (Kouro, 2010). All these features are possible due to its scalability and modularity, which is also important when it comes to maintenance, once it is easier to replace individual submodules in case of failure, then to replace the converter itself (Lesnicar, 2003).

Strategies to the current control in MMC are the same applied to two-level voltage source converters (VSCs), such as the decoupled dq reference frame control (Guan, 2011), the pq theory (Akagi, 2007) or using the model predictive control (MPC) (Cortés, 2008), which has been largely used recently due to its fast dynamic response, possibility to include the nonlinearities of the system and ease in digital implementation (Rodriguez, 2007), (Vargas, 2007), (Kouro, 2009) and (Perez, 2012). Besides current control, the MMC needs a proper voltage balancing technique in order to keep the submodule capacitors on their nominal voltage value. And also a circulating current control, to eliminate these current components generated from the voltage difference among the three phase legs, and which contains negative sequence components with the frequencies twice the fundamental one (Debnath, 2015).

Reference (Qin, 2012) proposed a control strategy based on the MPC algorithm. The method used there defined a cost function to control the ac-side currents, circulating currents and also to implement the capacitors voltage balancing task. However, it considered all possible C_n^{2n} switching states configurations, given a number of n submodules per arm, which would require higher computer effort as the number n of submodules increases.

Reference (Moon, 2015) proposed a MPC method with a reduced number of considered states for ac-side current control, capacitor voltage balancing control and circulating current control for a MMC. The developed method used three MPCs with different cost functions to each control goal.

This paper also proposes a MPC control strategy to regulate the ac-side currents and the circulating currents based on (Moon, 2015). However, the algorithm to implement the submodules capacitor voltage balancing task uses concepts of a sorting algorithm, like the one presented by (Saeedifard, 2010), together with the cost function idea used in MPC methods. Still, the control proposed methods not only reduces the required number of states in each cost function, but also reduces the computational load presented in common balancing tasks methods. Also, once MPC will be used, a discrete-time model of the MMC will be developed. At last, the simulation results will be presented in order to verify the effectiveness of the proposed MPC strategy applied to the case study system.

2 System Model and Control

2.1 MMC Topology and Mathematical Model

A diagram of the system in analysis is shown in Figure 1. The MMC consists of N = 4 half-bridge submodules per arm, resulting in a total of 24 submodules in the converter, and a reactance per arm (l_{arm}). Each half-bridge submodule consists of two IGBT switches with antiparallel diodes, and a capacitor. When the upper switch is turned on, the submodule capacitor voltage is applied to the terminals of the submodule. Otherwise, when the current flows through the lower switch, the voltage applied to the terminals is equal to zero, and the submodule is considered turned off.

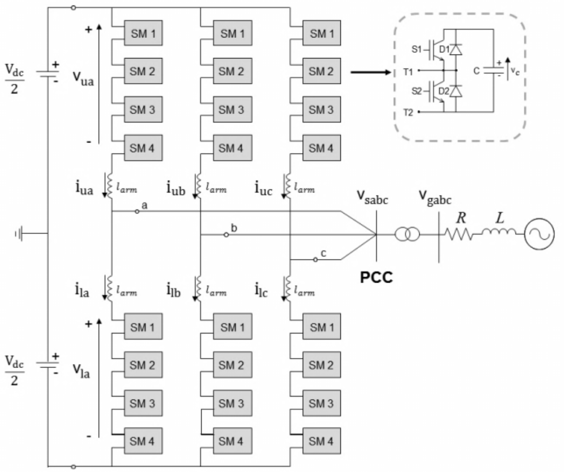

Figure 1. Distribution grid-connected MMC.

Based on Figure 1, the equations which govern phase-a are

$$\frac{V_{dc}}{2} - v_{ua} - l_{arm}\frac{di_{ua}}{dt} = Ri_a + L\frac{di_a}{dt} + v_{sa}, \quad (1)$$

$$\frac{V_{dc}}{2} - v_{la} - l_{arm}\frac{di_{la}}{dt} = -Ri_a - L\frac{di_a}{dt} - v_{sa}, \quad (2)$$

$$i_a = i_{ua} - i_{la}. \quad (3)$$

For phases b and c, the equations are identical. Also, the currents in the upper and lower arms can be calculated as follows

$$i_{ua} = \frac{i_a}{2} + \frac{i_{dc}}{3} + i_{za}, \quad (4)$$

$$i_{la} = -\frac{i_a}{2} + \frac{i_{dc}}{3} + i_{za}, \quad (5)$$

where i_{za} is the circulating current flowing through phase-a. Again, the equations for phases b and c are identical. These equations will be necessary to implement the MPC algorithm.

2.2 MPC Strategy for the ac-side Currents

The MPC Strategy is based on the discrete-time model of the system. Then it was used the Backward Euler approximation in the system equations as follows:

$$y_{t+T_s} = y_t + T_s f(y_{t+T_s}, t_{t+T_s}), \quad (6)$$

where T_s is the sampling period.

First, it is necessary to control the currents on the ac-side according to their reference values. In order to do that it is needed to predict the current value in the following step, each step. Combining (1), (2) and (3), it results in

$$v_{la} - v_{ua} = l_{arm}\frac{di_a}{dt} + 2Ri_a + 2L\frac{di_a}{dt} + 2v_{sa}. \quad (7)$$

Then, using (6), the predicted current can be calculated by

$$i_a(t+T_s) = \frac{1}{K}\Big(0.5 * \big(v_{la}(t+T_s) - v_{ua}(t+T_s)\big) - v_{sa}(t+T_s) + \frac{K_1}{T_s} i_a(t)\Big), \quad (8)$$

where $K_1 = \frac{l_{arm}}{2} + L$ and $K = \frac{K_1}{T_s} + R$. $v_{sa}(t+T_s)$ is the estimated grid voltage and can be approximated by the measured value of $v_{sa}(t)$. Also, the term $0.5*(v_{la}(t+T_s) - v_{ua}(t+T_s))$ corresponds to the predicted converter output voltage, $v_{out\_a}(t+T_s)$. Then, as the goal is to regulate the predicted current with respect to the reference one, then the first term in the cost function is

$$gi = abs\left(i_{aref}(t+T_s) - i_a(t+T_s)\right), \quad (9)$$

where abs(*) is the absolute value function.

From (9), if it is considered all possible combinations of switching states to determine the value of $v_{out}(t+T_s)$ in the cost function, the necessary number of combinations is C_N^{2N}, according to (Qin, 2012). In order to reduce this number, the approach based on (Moon, 2015) considers the possible voltage output levels N+1 instead, which is inside the range:

$$-\frac{N}{2}\frac{V_{dc}}{N} \le v_{out\_a}^* \le \frac{N}{2}\frac{V_{dc}}{N}. \quad (10)$$

Therefore, from the regulation of the ac-side currents, it is determined the necessary output voltage level, which can be expressed in terms of the lower and upper arm voltage output references

$$v_{ua}^* = \frac{V_{dc}}{2} - v_{out\_a}^* \quad (11)$$

$$v_{la}^* = \frac{V_{dc}}{2} + v_{out\_a}^* \quad (12)$$

which are inside the range

$$v_{ua}^*, v_{la}^* = \frac{V_{dc}}{N}[0, 1, \ldots, N]. \quad (13)$$

This algorithm to control the ac-side currents is summarized in the block diagram presented in Figure 2. But it is still necessary to control the circulating currents and the submodules capacitor voltages.

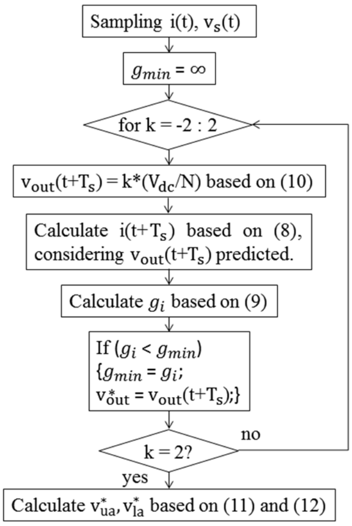

Figure 2. MMC-MPC ac-side currents control algorithm (N=4).

2.3 MPC Strategy for the Circulating Currents

This section presents the MPC algorithm used to minimize the circulating currents, which is important to reduce the submodules capacitor voltage ripples and converter losses.

The ac-side currents control, shown in the previous section, calculated a reference signal for the lower and upper arm output voltages. In the circulating current control method, these output voltage references are modified in order to accomplish this second goal of the overall control. Then, it is necessary to find an equation which relates the circulating current and the arms output voltages for a given phase-leg. First, (4) and (5) are added resulting in:

$$i_{za} = \frac{i_{ua}+i_{la}}{2} - \frac{i_{dc}}{3}. \quad (14)$$

Then, adding (1) and (2), and substituting (14), the dynamic of a MMC arm circulating current in terms of the arms output voltages is expressed as

$$l_{arm}\frac{di_{za}}{dt} = \frac{V_{dc}}{2} - \frac{v_{la}+v_{ua}}{2}. \quad (15)$$

Using the Euler approximation equation (6) in (15), it is obtained the discrete equation need to control the circulating current component in each phase, and already considering the reference voltages calculated previously

$$i_{za}(t+T_s) = \frac{T_s}{2l_{arm}}\left(V_{dc} - v^*_{la}(t+T_s) - v^*_{ua}(t+T_s)\right) + i_{za}(t). \quad (16)$$

However, according to (Moon, 2015), it is needed to add a voltage level V_{za} in each arm output voltage in order to control the circulating current components. This level addition does not interfere in the converter output voltage $v^*_{out\_a}$, nor does it in the ac current i_a. It only appears in the circulating component equation as shown bellow

$$i_{za}(t+T_s) = \frac{T_s}{2l_{arm}}\{V_{dc} - [(v^*_{la}(t+T_s) + V_{za}) + (v^*_{ua}(t+T_s) + V_{za})]\} + i_{za}(t). \quad (17)$$

In this paper, only two voltage levels are allocated to V_{za}, and so this voltage component can assume the values

$$V_{za} = \frac{V_{dc}}{N}[-1, 0, 1]. \quad (18)$$

The cost function for the circulating current components has the goal to minimize its components values, and so can be defined as

$$gz = abs\left(i_{za}(t+T_s)\right). \quad (19)$$

Then the voltage references for the upper arm and lower arm, considering the circulating current control, are

$$v^*_{ua\_z} = v^*_{ua}(t+T_s) + V^*_{za} \quad (20)$$
$$v^*_{la\_z} = v^*_{la}(t+T_s) + V^*_{za} \quad (21)$$

which are inside the range

$$v^*_{ua\_z}, v^*_{la\_z} = \frac{V_{dc}}{N}[0, 1, .., N]. \quad (22)$$

This algorithm to control the circulating current components is summarized in the block diagram presented in Figure 3.

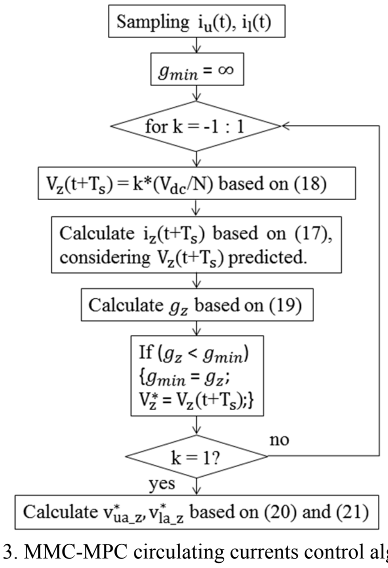

Figure 3. MMC-MPC circulating currents control algorithm.

2.4 Submodule Capacitor Voltage Balancing

Similar to other multilevel converter topologies, the MMC needs an active voltage balancing strategy in order to maintain the submodule capacitor voltages regulated at their nominal value V_{dc}/N. The most widely accepted voltage balancing strategy is based on a sorting method (Debnath, 2015).

To perform the voltage balancing task based on a sorting method, it is necessary to measure all capacitors voltages, and sort them, and the upper and lower arms currents. Then, if the upper (lower) arm current is positive, a determined number of submodules $\mathrm{Nu_{on}}$ ($\mathrm{Nl_{on}}$) with the lowest voltages are inserted, and the submodules are charged. On the other hand, if the upper (lower) arm current is negative, a determined number of submodules $\mathrm{Nu_{on}}$ ($\mathrm{Nl_{on}}$) with the highest voltages are inserted, and the submodules are discharged. Regardless of the direction of the arm current, if a submodule is bypassed, the corresponding capacitor voltage remains the same. Although the sorting method guarantees a proper capacitor voltage balancing, it produces unnecessary switching transitions and it is necessary to implement the sorting algorithm for each leg every sampling period. Then, as higher the number of submodules, higher is the computing time to implement this task.

This paper proposes a balancing task which uses both concepts of a sorting algorithm, but without implementing the complete sorting every sampling time, and a MPC control where a cost function is used. However, it is proved that in the method proposed it is not necessary to predict the submodule capacitor voltage to accomplish it.

To determine whether the submodule is on/off, it is used the voltage references calculated previously as shown as follows

$$Nu_{on} = \frac{v^*_{ua\_z}}{V_{dc}/N} = [0, 1, .., N], \quad (23)$$

$$Nl_{on} = \frac{v^*_{la\_z}}{V_{dc}/N} = [0, 1, .., N]. \quad (24)$$

Then, instead of using the exact number of submodules to be turned on/off, it is used the variation $\Delta\mathrm{Nu_{on}}$ and $\Delta\mathrm{Nl_{on}}$ in order to avoid unnecessary switching transitions and computational time. Then, if $\Delta\mathrm{Nu_{on}}, \Delta\mathrm{Nl_{on}} > 0$, the submodules whose switching states are off are analyzed based on a cost function gc, that is presented as follows, and the minimum value is chosen. However, if $\Delta\mathrm{Nu_{on}}, \Delta\mathrm{Nl_{on}} < 0$, the submodules whose switching states are on are analyzed based on a cost function gc and the maximum value is chosen.

The cost function gc is usually based on the predicted values of the capacitor upper and lower voltages, which can be calculated based on the predicted switched-on/off submodules, according to

$$V_{cna}(t + T_s) = V_{cna}(t) + T_s \frac{i(t)}{C}, \quad (25)$$

where n is the number of the submodule per phase and $\mathrm{i(t)}$ will be equal to $\mathrm{i_{ua}(t)}$ or $\mathrm{i_{la}(t)}$ to the submodules in the upper arm or lower arm, respectively, if the submodules are on. If the submodule is turned off, then the term referred to the current in (25) is equal to zero. And the cost function is usually given by the absolute value of the sum of the submodules predicted capacitor voltages. However, when using this cost function it is necessary to consider all possible switching states. To avoid it and reduce the number of possible switching states to be considered, only one submodule is selected at each loop and the number of loops is determined by the value of $\Delta\mathrm{Nu_{on}}, \Delta\mathrm{Nl_{on}}$. The cost function used to compare them, based on the concepts of the sorting method explained previously, is given by

$$gc = i(t)(V_{cna}(t + T_s) - \tfrac{V_{dc}}{N}), \quad (26)$$

where the current is multiplied to determine whether the submodule is charging or discharging, if its value is positive or negative, respectively.

However, the algebraic difference between the submodule capacitor voltage and its nominal value is being used, instead of the absolute value. And to always choose the minimum value of gc, (26) can be simplified based on the inequalities:

$$\text{if } a \lesseqgtr b, \text{ then } a + c \lesseqgtr b + c, \ \forall c, \quad (27)$$

$$\text{if } \mathrm{z} \gtreqless 0 \text{ and if } a < b, \text{ then } za \lesseqgtr zb. \quad (28)$$

And so, the new cost function is given by

$$gc = \mathrm{dec} * i(t) V_{cna}(t + T_s), \quad (29)$$

where dec = +/-1, for $\Delta\mathrm{Nu_{on}}, \Delta\mathrm{Nl_{on}} \geq 0/< 0$.

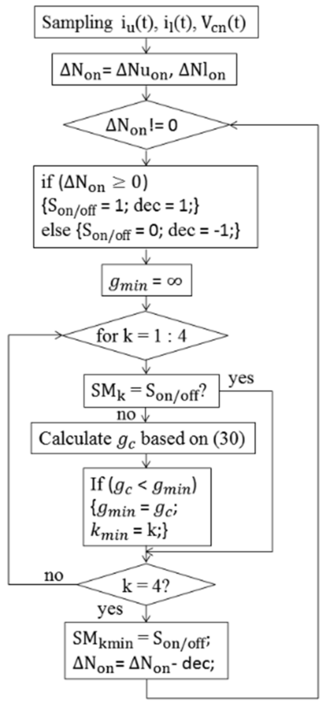

Figure 4. Submodule capacitor voltage balancing algorithm (N=4).

Still, as the submodules to be turned on and off are compared separately, the current term in equation (25), used to compare the submodules to be turned on, does not interfere in the comparison, as shown in equation (27), and gc can be even more simplified to

$$gc = \mathrm{dec} * [i(t) V_{cna}(t)], \quad (30)$$

proving that the predicted values of the capacitors voltages are not necessary. Then, the number of computational operations is reduced, just as the number of considered switching states. At last, the capacitors voltage balancing method presented is summarized in Figure 4.

2.5 Control of a grid-connected MMC

As mentioned in the Introduction section, there are different methods presented in the literature to calculate the reference currents used in the MPC algorithm exposed previously. This paper proposes the utilization of the pq theory (Akagi, 2007) together with the αβ-frame.

According to the pq theory, the real and imaginary power can be calculated as follows

$$p = v_\alpha i_\alpha + v_\beta i_\beta, \tag{31}$$
$$q = v_\beta i_\alpha - v_\alpha i_\beta. \tag{32}$$

Then, the currents in αβ-frame are calculated as

$$i_\alpha = p\frac{v_\alpha}{{v_\alpha}^2+{v_\beta}^2} + q\frac{v_\beta}{{v_\alpha}^2+{v_\beta}^2}, \tag{33}$$
$$i_\beta = p\frac{v_\beta}{{v_\alpha}^2+{v_\beta}^2} - q\frac{v_\alpha}{{v_\alpha}^2+{v_\beta}^2}. \tag{34}$$

After calculating the reference currents, given a specified p and q, it is then transformed these αβ-frame reference values to the abc-frame using matrix K.

$$K = \sqrt{\frac{2}{3}}\begin{bmatrix} 1 & 0 \\ -\frac{1}{2} & \frac{\sqrt{3}}{2} \\ -\frac{1}{2} & -\frac{\sqrt{3}}{2} \end{bmatrix}, \tag{35}$$
$$i_{abc} = K i_{\alpha\beta}. \tag{36}$$

A complete scheme of this control is shown in the block diagram of Figure 5.

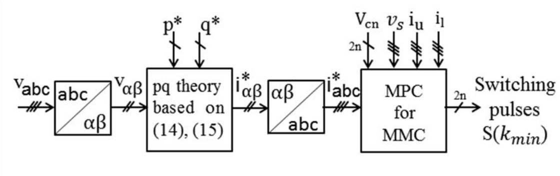

Figure 5. Block diagram of the system control scheme.

3 Simulation Results

In this section the performance of the system in analysis, shown in Figure 1 and whose parameters are given in Table 1, is evaluated. Simulations were conducted in the environment of circuit simulation PSIM, and the results proving the MPC control capability of controlling the ac-side currents, circulating current components and maintaining the submodules capacitor voltages balanced are shown. The simulation routine starts in standby mode, which means that real and imaginary power references are equal to zero, and submodules capacitors are already charged to their nominal values.

Table 1. System Parameters.

Parameter	Value
MMC nominal power	5 kVA
Nominal frequency	60 Hz
Transformer (150 kVA)	13.8 kV/220 V
Transformer leakage reactance	3.5%
R	2 Ω
L	15 mH
l_{arm}	5 mH
Submodule capacitor C	6mF
DC Source Voltage	500 V
Sampling period	50 µs

At t = 0.2 s a power transfer command from dc side to ac is activated and its reference value is p^* = 5 kW, in this case, imaginary power is kept q^* = 0. Then, at t = 2.5 s the real power reference suffers a step change to p^* = 7 kW value, while q^* is again maintained the same. At last, when simulation time reaches t = 3 s, imaginary power reference is step changed to q^* = -4 kW, whereas real power reference is kept with p^* = 7 kW value. Simulation results for this routine are shown in Figure 6.

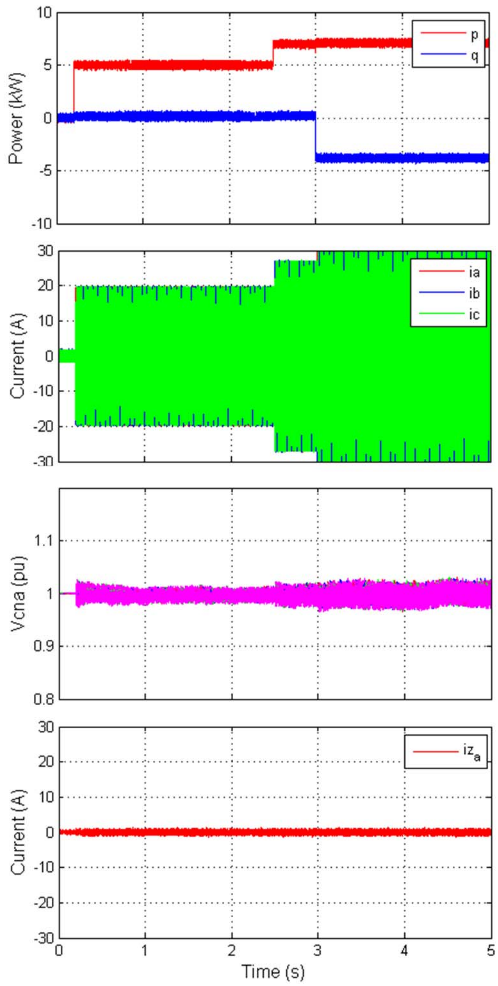

Figure 6. Simulation results: (a) real and imaginary power components of the grid-connected MMC; (b) ac-side currents of the MMC; (c) submodules capacitor voltages of MMC phase-a; and (d) circulating current component of phase-a.

Figure 6(a) illustrates real and imaginary power components and the control capability of regulating them to their reference values. Figure 6(b) and (c) show the ac-side currents of the MMC, controlled to their reference values, and phase–a submodule capacitor voltages of the MMC balanced to their nominal value. At last, Figure 6(d) shows the circulating current component minimized.

When real time practical implementation is desired, problems related to the delay between signals acquisition and the effective commutation of the switches may occur due to the execution time of control algorithms. In order to evaluate this matter, simulations considering delays in switching command signals were implemented, and it was not observed instability problems for delays up to half of the controllers' sampling period. However, it requires that the execution time of control algorithms is limited to intervals of that magnitude. To overcome this limitation when the MMC has a high number of submodules, it may be necessary to implement the controllers in a hardware structure capable of parallelizing the execution, such as FPGA.

4 Conclusion

This paper proposes two MPC strategies, one to control the ac-side currents components and other to minimize the circulating current components. Also, it proposes a capacitor voltage balancing algorithm based on both sorting and MPC methods. The three of them together have shown to be very efficient, accomplishing the goals defined for each one. Besides, they need a reduced number of switching possibilities and less computational effort, which is extremely important for real time experimental implementation.

References

Akagi, H., Watanabe, E., H. and Aredes, M. (2007). Instantaneous power theory and applications to power conditioning (Vol. 31). John Wiley and Sons.

Cortes, P., Kazmierkowski, M., P., Kennel, R., M., Quevedo, D., E. and Rodriguez, J. (2008). Predictive control in power electronics and drives. IEEE Transactions on Industrial Electronics, Vol. 55, No. 12, pp. 4312-4324.

Debnath, S., Qin, J., Bahrani, B., Saeedifard, M. and Barbosa, P. (2015). Operation, Control, and Applications of the Modular Multilevel Converter: A Review. PowerTech Conference Proceedings. IEEE Transactions on Power Electronics, Vol. 30, No. 1, pp. 37-53 Jan. 2015.

Guan, M., Xu, Z., and Chen, H. (2011). Control and modulation strategies for modular multilevel converter based HVDC system. In IECON 2011-37th Annual Conference on IEEE Industrial Electronics Society, pp. 849-854.

Kouro, S., Cortes, P., Vargas, R., Ammann, U. and Rodriguez, J. (2009). Model predictive control a simple and powerful method to control power converters. IEEE Trans. Ind. Electron., Vol. 56, No. 6, pp. 1826-1838.

Kouro, S., Malinowski, M., Gopakumar, K., Pou, J., Franquelo, L., G., Wu, B., Rodriguez, J., Perez, M. and Leon, J., I. (2010). Recent advances and industrial applications of multilevel converters. IEEE Trans. Ind. Electron., Vol. 57, No. 8, pp. 2553-2580.

Lesnicar, A. and Marquardt, R. (2003). An innovative modular multilevel converter topology suitable for a wide power range. (IEEE, Ed.) PowerTech Conference Proceedings. IEEE Bologna, Vol. 3, 23-26 June 2003.

Moon, J., Gwon, J., Park, J., Kang, D. and Kim, J. (2015). Model Predictive Control With a Reduced Number of Considered States in a Modular Multilevel Converter for HVDC System. IEEE Trans. On Power Delivery, Vol. 30, No. 2, pp. 608-617 April 2015.

Perez, M., A., Rodriguez, J., Fuentes, E. and Kammerer, F. (2012). Predictive control of ac-ac modular multilevel converters. IEEE Trans. Ind. Electron., Vol. 59, No. 7, pp. 2832-2839.

Qin, J. and Saeedifard, M. (2012). Predictive control of a three-phase dc-ac modular multilevel converter. IEEE Energy Conversion Congress and Exposition, pp. 3500-3505.

Rodriguez, J., Lai, J. and Peng, F., Z. (2002). Multilevel inverters: A survey of topologies, controls, and applications. IEEE Transactions on Industrial Electronics, Vol. 49, No. 4, pp. 724-738.

Rodriguez, J., Pontt, J., Silva, C., A., Correa, P., Lezana, P., Cortes, P. and Ammann, U. (2007). Predictive current control of a voltage source inverter. IEEE Trans. Ind. Electron., Vol. 54, No. 1, pp. 495-503.

Saeedifard, M. and Iravani, R. (2010). Dynamic Performance of a Modular Multilevel Back-to-Back HVDC System. IEEE Trans. On Power Delivery, Vol. 25, No. 4, pp. 2903-2912 Oct. 2010.

Vargas, R., Cortes, P., Ammann, U., Rodrigues, J. and Pontt, J. (2007). Predictive control of a three-phase neutral-point-clamped inverter. IEEE Trans. Ind. Electron., Vol. 54, No. 5, pp. 2697-2705.